Heliyon 10 (2024) e32500

Contents lists available at ScienceDirect

Heliyon

journal homepage: www.cell.com/heliyon

Research article

Assessment of wind energy resource in the western region of Somaliland

Shaima Batran [a], Mohamed Jama [a,*], Jawad Yousaf [a], Taimur Hassan [a], Mohammed Ghazal [a], Hazlie Bin Mokhlis [b]

[a] Department of Electrical, Computer and Biomedical Engineering, Abu Dhabi University, Abu Dhabi, United Arab Emirates
[b] Department of Electrical Engineering, University of Malaya, Kuala Lumpur, Malaysia

ARTICLE INFO

Keywords:
Wind energy
Techno-economic assessment
Wind turbine
Renewable energy
Resource
Levelized cost of electricity
Weibull distribution function
Maximum likelihood estimation

ABSTRACT

As the population of Somaliland continues to grow rapidly, the demand for electricity is anticipated to rise exponentially over the next few decades. The provision of reliable and cost-effective electricity service is at the core of the economic and social development of Somaliland. Wind energy might offer a sustainable solution to the exceptionally high electricity prices. In this study, a techno-economic assessment of the wind energy potential in some parts of the western region of Somaliland is performed. Measured data of wind speed and wind direction for three sites around the capital city of Hargeisa are utilized to characterize the resource using Weibull distribution functions. Technical and economic performances of several commercial wind turbines are examined. Out of the three sites, Xumba Weyne stands out as the most favorable site for wind energy harnessing with average annual power and energy densities at 80 m hub height of 317 kW/m^2 and 2782 kWh/m^2, respectively. Wind turbines installed in Xumba Weyne yielded the lowest levelized cost of electricity (LCOE) of not more than 0.07 $/kWh, shortest payback times (i.e., less than 7.2 years) with minimum return on investment (ROI) of approximately 150%.

1. Introduction

Over the past 10 years, the installed worldwide capacity of wind energy has increased threefold. In 2022, the world's total installed wind energy capacity has reached to approximately 900 GW, accounting for nearly 27% of the total installed renewable energy capacity in the world [1]. Benefiting from the significant improvements in wind turbine technologies, wind farm scale efficiency, construction and procurement costs [2]. This has resulted in competitive levelized cost of electricity (LCOE), plummeting in 2021 by 61.6% and 53.4% for onshore and offshore wind energy, respectively [2]. From 2010 to 2022, the global weighted average LCOE dropped by 69%, from $0.107 per kWh to $0.033 per kWh [3]. Despite the rapid growth in this renewable energy sector, African countries have yet to tap into the massive wind energy potential in the continent, with less than 1% share of the global installed wind energy capacity in 2022 [1].

Various scholars worldwide have studied wind energy potential both technically and economically. In Australia [4], Weibull distribution is deployed to model the wind energy resource in three sites. Few studies assessed wind energy potential in Iran. For example, the authors in [5], conducted a techno-economic assessment of wind energy examining four wind turbine models for the

* Corresponding author.
E-mail address: mohamed.jama@adu.ac.ae (M. Jama).

https://doi.org/10.1016/j.heliyon.2024.e32500
Received 16 March 2024; Received in revised form 10 May 2024; Accepted 5 June 2024

Available online 13 June 2024

east of Iran. Similar study has investigated the wind resource potential in four locations in Sistan and Balouchestan provinces in Iran [6]. Technical and economical assessment of wind energy resource in seven different cities in Jordan using measured wind speed data has been reported in [7]. Numerous relevant research attempts were conducted in Pakistan to evaluate the potential of wind energy in various parts of the country. In [8], wind energy assessment is carried out for two locations in Sindh provinces of Pakistan. The study encompassed statistical analysis of measured wind data, Weibull distribution function parameter estimation, power and energy densities calculations for various wind turbine models. Another work focused on evaluating the wind resource potential along the coastline of Pakistan [9]. The authors in [10], assessed the potential of wind energy at the Southeastern province city of Hyderabad. Weibull and Rayleigh distribution functions were employed to characterize the wind potential on the annual, monthly, and seasonal time frames. On the other hand, the authors in [11], utilized a new method to evaluate wind energy potential in southern Punjab, Pakistan, by applying the Weibull distribution function model. Twelve sites located in the northern, central, and southern regions of Saudi Arabia have been examined for wind energy potential [12]. Ten different coastal and offshore locations were assessed for wind energy potential in the State of Kuwait [13]. Techno-economic wind resource analysis has been conducted for the central region in Thailand as reported in [14]. The authors recommended Vestas V60-850 kW as the most economic commercial wind turbine for regions with moderate wind resource. In Malaysia, researchers have analyzed the cost of wind turbines and their economic viability in rural areas [15]. In [16], the feasibility of extracting wind energy in the Caribbean region of Colombia using 10-min resolution wind data is investigated. The authors in [17] deployed Weibull distribution functions to estimate the yearly mean wind speeds in Beibu Gulf of China at 100 m above sea level for a duration of eight years. The study revealed that December and July had the most potential for wind. In [18], wind energy resource is estimated from 2007 to 2013 using Weibull functions in west of Cameroon. The authors tested various Weibull parameters estimation techniques where maximum likelihood method was found to be the most effective. The authors in [19], assessed wind energy using Vergnet 275 kW wind turbine in three different locations in Fiji. In India, Weibull distribution functions were fitted into measured wind speed in specific regions [20]. The potential of wind energy was assessed in Serbia's Knjazevac Municipality, where the authors concluded that only one area of the municipality is suitable for wind collection at a height of 100 m [21]. Researchers in the Republic of Korea have conducted an assessment using 10-year long wind data employing the Weibull model [22]. In [23], wind potential in the Moroccan coastal districts from 2015 to 2018 was examined. The authors' findings showed that the maximum wind speeds were observed in the summer at a height of 50 meters. In [24], wind energy potential in 50 different regions in Bangladesh is investigated. A comprehensive study involving technical, economic, and environmental assessment of small-scale wind turbines in the Gaza Strip is proposed in [25].

Located in the Horn of Africa, Somaliland is recognized as one of most favorable spots for harnessing wind energy in Africa [26]. Despite its undeniable potential, wind energy is far from being mainstream in Somaliland. According to IRENA, the total installed wind energy capacity in Somalia is a modest 4 MW, all being onshore wind energy capacity [1]. The electricity sector in Somaliland is comprised of high speed diesel generators (HSDG) run mini-grids operated by private energy service providers (ESPs) with total power capacity of 150 MW [27]. In addition to the high prices of imported diesel fuel, these mini-grids suffer from substantial losses due to the lack of synchronization between HSDGs, poor operation and maintenance practices, and shortage of trained technicians [28]. All of these factors have resulted in having over-inflated electricity tariffs in Somaliland with a weighted average of 0.68 $/kWh and a maximum value that can reach up to 0.9 $/kWh in some locations [28]. These excessive electricity prices have depleted household income and hindered sustainable economic development. Currently, renewable energy sources make up 16.2% of the total installed power capacity in Somaliland, the vast majority being solar photovoltaic (PV) power [27]. Increasing the penetration of renewable energy (particularly solar PV and wind energy), would reduce the needed capacity from HSDGs, facilitating substantial reduction in the electricity prices and stabilizing the electricity market in the long run. To achieve an optimum balance between thermal power units and renewable energy sources, a deep understanding of the available renewable energy resource is essential. Wind energy, for instance, has not received enough attention from both the public and private sectors. Furthermore, in depth technical and economic assessment studies are noticeably absent in the research community in Somaliland.

In this work, a thorough techno-economic assessment of the wind energy resource in three sites located at the western region of Somaliland is conducted. To the best of our knowledge, this is the first study of its kind to address this topic in Somaliland and possibly in the Somali Peninsula. Measured wind speed and wind direction data collected from three weather stations in Aburin, Daarbuduq, and Xumba Weyne, are utilized to characterize the wind resource at various time scales. Weibull distribution function is used to model the magnitude and the variability of the wind resource in the three locations with its shape and scale parameters being estimated using various estimation techniques such as graphical method (GM), maximum likelihood estimation (MLE), etc. The wind potential is assessed by statistically estimating the sites' power and energy densities. The technical performances of numerous commercial wind turbines with varying technical specifications are analyzed in terms of their annual energy yield and capacity factor. Furthermore, the economic feasibility of the investigated wind turbines is examined by estimating the levelized cost of electricity (LCOE) throughout the turbines' lifespan. Finally, a concise sensitivity analysis is performed to examine the turbines' economic performance in response to uncertainties in key technical and economic factors.

The paper is organized as follows: Section 2 includes the materials and methodology. Section 3 entails the results and discussions of the key research findings. Conclusions are drawn in Section 4.

2. Materials and methods

This study focuses on assessing the wind energy potential in three sites located in the western region of Maroodi Jeex, Somaliland. The three investigated sites are Aburin, Daarbuduq, and Xumba Weyne as shown in Fig. 1. In this section, the analysis method utilized

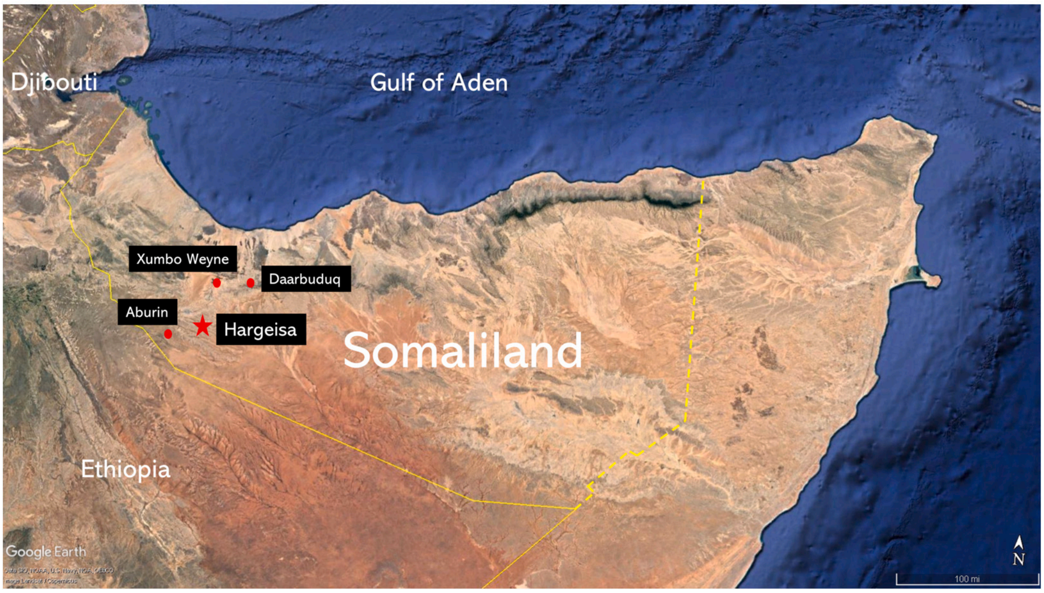

Fig. 1. Somaliland map showing the measurement sites, adapted from Google Earth (2024).

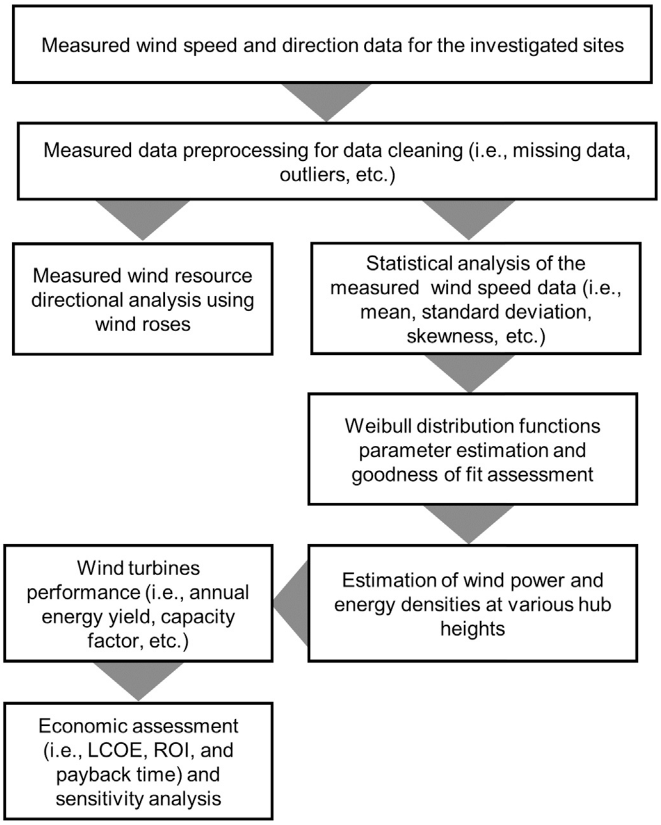

Fig. 2. Methodology flowchart.

in this study is thoroughly discussed. This includes statistical analysis of the wind resource and a comprehensive analysis of wind turbine technical and economic performances in the investigated sites. Fig. 2 summarizes the adopted research methodology.

Table 1
General information of the studied sites.

Site	Region	Longitude	Latitude	Elevation (m)	Data Period
Aburin	Maroodi Jeex	9°31'3" N	43°48'21" E	1462	7/3/2011-6/3/2012
Xumbo Weyne	Maroodi Jeex	09°53'15" N	44°19'17" E	933	7/3/2011-6/3/2012
Daarbuduq	Maroodi Jeex	09°51'14" N	44°32'08" E	949	7/3/2011-6/3/2012

2.1. Study area and measured data overview

The selected sites are at close proximity to the capital and the most densely populated city of Hargeisa. Table 1 demonstrates the geographic location and altitude of the three sites. The investigated sites are characterized as plateau landscape with semi-arid climate [29]. The annual average temperatures range from 20 - 24 °C with total annual precipitation of 500-600 mm [30]. Somaliland generally feature two wind regimes as a result of the interannual transition of the intertropical convergence zone (ITCZ), the first is north-easterly winds and the second is south-westerly winds. As for the vegetation in the investigated sites, it ranges from sparse drought resistant scrubs to more dense scrublands and grasslands, particularly over the mountainous landscapes such as Aburin [31]. Hourly measured wind speed and direction data spanning from 7/3/2011 to 6/3/2012 were deployed in this study. The data were recorded at typical height of 10 m in ground weather stations located at the three sites as part of the Somali Water and Land Management (SWALIM) project run by Food and Agriculture Organization (FAO) of the United Nations [32]. The raw data obtained from SWALIM weather data repositories suffered from sufficient discontinuities and anomalies, requiring substantial data pre-processing. This data quality concern has restricted the research to utilizing a single year worth of the most reliable data of wind speed and direction for the three sites under study. The wind speed and wind direction data have gone pre-processing procedure to treat the missing or corrupt data using nearest neighbor interpolation method [33,34]. Three wind turbine hub heights are deployed in this study, namely 30 m, 50 m, and 80 m. This specific selection of hub heights can be justified considering the specific needs of Somaliland energy market. Small to medium sized wind turbines with hub heights lower than 50 m could be a natural fit for urban and semi-urban installations, potentially serving distributed micro-grid based electric network which is the case in Somaliland. Knowing that small to medium urban and semi-urban wind turbines could be a natural choice for Somaliland energy market and distributed micro-grid based electric network. On contrary, analysis involving high hub heights, such as 80 m, is in alignment with the general world trend of deploying taller wind turbines with megawatt-scale power capacity in large-scale wind energy farms, which could be a future consideration for Somaliland.

2.2. Wind resource probability functions

The two-parameter Weibull distribution has been used to model the probability of the measured wind speeds over various time scales, such as seasonal, monthly, diurnal, and hourly and numerous turbine hub height. The Weibull probability density function (PDF) and commutative distribution function (CDF) can be mathematically represented as function of wind speed, v, as follows [35]:

$$f(v) = \left(\frac{k}{c}\right)\left(\frac{v}{c}\right)^{k-1} exp\left[-\left(\frac{v}{c}\right)^{k}\right], \tag{1}$$

$$F(v) = 1 - exp\left[-\left(\frac{v}{c}\right)^{k}\right], \tag{2}$$

where $f(v)$ and $F(v)$ represent the Weibull's PDF and CDF. The parameters k and c are the distribution function shape and scale parameters, respectively. Using the estimated Weibull distribution parameters, wind speed mean, v_m, and standard deviation, σ, can be calculated as [6]

$$v_m = c\Gamma\left(1+\frac{1}{k}\right), \tag{3}$$

$$\sigma = c\sqrt{\left(\Gamma\left(1+\frac{2}{k}\right) - \Gamma^2\left(1+\frac{1}{k}\right)\right)}, \tag{4}$$

where $\Gamma(*)$ is the Gamma function and it can be approximated using the following fifth order polynomial as follows [36]:

$$\Gamma(x) = 0.1226x^5 - 1.1149x^4 + 3.9489x^3 - 6.3653x^2 + 4.3941x. \tag{5}$$

Similarly, the most frequent wind speed, v_f, and the most energetic wind speed, v_e, can be approximated using the Weibull's distribution parameters as follows [37]

$$v_f = c\left(\frac{k-1}{k}\right)^{\frac{1}{k}}, \tag{6}$$

$$v_e = c\left(\frac{k+2}{k}\right)^{\frac{1}{k}}. \tag{7}$$

2.3. Weibull distribution parameters estimation

In this study, four different Weibull distribution parameters estimation methods have been used, namely graphical method, maximum likelihood estimation method, empirical method, and energy pattern factor method.

2.3.1. Graphical method (GM)

The graphical method evaluates the wind data by fitting a linear representation for wind speed, v, data using the least squares method [38], the method expression as the following [38]:

$$\ln[-\ln(1-F(v))] = k\ln v - k\ln c, \tag{8}$$

$$y = \ln[-\ln(1-F(v))], \tag{9}$$

$$x = \ln v, a = k, b = -k\ln c, \tag{10}$$

where $F(v)$ represents the cumulative distribution function. The parameters a and b represent the slope and the y-intercept, respectively. The two Weibull parameters can be expressed as function of a and b using [36]

$$k = a, \tag{11}$$

$$c = e^{-\frac{b}{k}}. \tag{12}$$

2.3.2. Maximum likelihood estimation (MLE)

This statistical parameter estimation method is widely used in estimating the parameters of probability density functions. In the context of Weibull distribution function, this method aims at maximizing the likelihood function assuming the observed wind speed data are the most probable. The estimated values of k and c can be evaluated using the following relations [8],

$$k = \left(\frac{\sum_{i=1}^{T} v_i^k ln(v_i)}{\sum_{i=1}^{T} v_i^k} - \frac{\sum_{i=1}^{T} ln(v_i)}{T} \right)^{-1}, \tag{13}$$

$$c = \left(\frac{1}{T} \sum_{i=1}^{T} v_i^k \right), \tag{14}$$

where T is the number of occurrences in the wind speed data that are not zero, and v_i is the wind speed value at time i.

2.3.3. Empirical method (EM)

This method is a relatively simple method that is readily applied on the measured wind speed data [18]. Using the statistical mean, $\overline{v}$ and standard deviation, σ, of the wind speed data, the Weibull parameters can be calculated as

$$k = \left(\frac{\overline{v}}{\sigma} \right)^{-1.086}, \tag{15}$$

$$c = \frac{\overline{v}}{\Gamma\left(1 + \frac{1}{k}\right)}. \tag{16}$$

2.3.4. Energy pattern factor (EPF)

This method also utilizes the statistical mean of the wind speed data to determine the two Weibull parameters, k and c, which can be calculated using the following formulas [18]:

$$E_{pf} = \frac{\overline{v^3}}{\overline{v}^3}, \tag{17}$$

$$k = 1 + \frac{3.69}{E_{pf}^2}, \tag{18}$$

$$c = \frac{\overline{v}}{\Gamma\left(1 + \frac{1}{k}\right)}, \tag{19}$$

where Γ is the gamma function and E_{pf} is the energy pattern factor.

2.4. Goodness of fit metrics

Various statistical metrics have been deployed to assess the goodness of fit of the aforementioned estimation techniques used to estimate the Weibull distribution parameters. This includes root mean square error (RMSE), mean absolute percentage error (MAPE), relative root mean square error (RRMSE), mean bias error (MBE), and the coefficient of determination (R^2) [8]. Root mean square error (RMSE)is calculated as follows:

$$RMSE = \sqrt{\frac{1}{N}\sum_{i=1}^{N}\left(v_i - \hat{v}_i\right)^2}, \tag{20}$$

where v_i and $\hat{v}_i$ are the ith sample of the measured and estimated wind speed. Whereas N is the total number of wind speed samples. Positive and smaller values of RMSE indicates closer alignment between the actual wind speed data and the Weibull estimated values. A closely related statistical metric is RRMSE, which is the normalized version of RMSE. Values of RRMSE lower than 10% are desirable. Another metric is MAPE which evaluates the accuracy of the estimated wind speed value compared to their actual counterparts. MAPE can be calculated using the following formula [8]:

$$MAPE = \frac{1}{N}\sum_{i=1}^{N}\left|\frac{v_i - \hat{v}_i}{v_i}\right| \times 100. \tag{21}$$

To evaluate whether the estimated Weibull function overestimates or underestimates, MBE is calculated as follows [8]:

$$MBE = \frac{1}{N}\sum_{i=1}^{N}\left(v_i - \hat{v}_i\right), \tag{22}$$

where values of positive values of MBE indicate overestimation, while negative values indicate underestimation. The strength of correlation between the actual wind speed values and the estimated ones can be also gauged using the coefficient of determination (R^2), which is evaluated as

$$R^2 = 1 - \frac{\sum_{i=1}^{N}\left(v_i - \hat{v}_i\right)}{\sum_{i=1}^{N}\left(v_i - \bar{v}\right)}. \tag{23}$$

Values of R^2 closer to one signifies better fit of the estimated Weibull function to the actual wind speed data.

2.5. Wind power and energy densities

The average wind power, P_w, is proportional to the cube of the average wind speed, v, as described by

$$P_w = \frac{1}{2}\rho A_r v^3, \tag{24}$$

where ρ is the air density in kg/m^3 at sea level, which is 1.225 kg/m^3 at atmospheric pressure of 1 atm and ambient temperature of 25 °C. Whereas A_r is the wind turbine rotor swept area in m^2 [5]. The corresponding average wind power density P_D in W/m^2 can be expressed as

$$P_D = \frac{P_w}{A_r} = \frac{1}{2}\rho v^3. \tag{25}$$

Equation (25) does not incorporate the frequency of occurrences of wind speed at a specific cite. More practical representation of P_D is to use the Weibull distribution function as follows [6]:

$$P_D = \frac{P_w}{A_r} = \frac{1}{2}\rho\int_0^\infty v^3 f(v)dv = \frac{1}{2}\rho c^3\Gamma\left(1+\frac{3}{k}\right), \tag{26}$$

Air density ρ is a function of the air temperature and pressure. Temperature and pressure are influenced by elevation above the sea level [35]. The density of the air can be calculated using the ideal gas law,

$$\rho = \frac{p}{RT} = 3.4837\frac{p}{T}, \tag{27}$$

where p is the air pressure in kPa, R is the gas constant, and T is temperature in Kelvin (K). The atmospheric pressure up to 5000 meters is expressed as [35]:

$$p = 101.29 - (0.011837)z + (4.793\times10^{-7})z^2, \tag{28}$$

where z is the elevation above the sea level measured in m. The wind energy density E_D in Wh/m^2 can be calculated by multiplying the wind power density evaluated in Equation (26) by the desired time period, T, as shown in the following expression [5]:

$$E_D = P_D T = \frac{1}{2}\rho c^3\Gamma\left(1+\frac{3}{k}\right)T. \tag{29}$$

Table 2
Characteristics of the selected wind turbines [7,8].

Wind Turbine	Model	P_r (kW)	Rotor diameter (m)	Hub height (m)	v_{ci}, v_r, v_{co} (m/s)	Initial cost ($/kW)
WT1	Vestas V100	1800	100	80	4,12,20	1274
WT2	Dewind D6	1250	64.3	60	3,13,23	1743
WT3	Enercon E53/800	800	52.9	60	3,12,34	1743
WT4	Enercon E40/600	600	40	50	2.5,12,28	4358
WT5	Enercon E58/1000	1000	58.6	70	2.5,12,28	1743
WT6	Dewind D8	2000	80	80	2.5,13,25	1743
WT7	Enercon E66/1500	1500	70	86	2.5,13,25	2905
WT8	S47-660	660	47	40	4,15,25	1000

2.6. Wind turbine performance

To estimate the wind turbine annual energy yield, the measured wind velocity profile needs to be extrapolated vertically to the actual turbine hub height. This can be achieved by the power law method as depicted below [13],

$$\frac{v}{v_r} = \left(\frac{z}{z_r}\right)^{\alpha}, \tag{30}$$

where v represents the wind velocity at the intended turbine hub height z, while v_r represents the measured wind speed at the reference height z_r (typically z_r is 10 m). The exponent α is the shear coefficient, which is a dimensionless value that varies depending on the elevation, atmospheric conditions across the day and the type of terrain where the turbines are installed [39]. The parameter α can be approximated using the following empirical relation as follows [38]:

$$\alpha = \frac{0.37 - 0.088\ln(v_r)}{1 - 0.088\ln\left(\frac{z_r}{10}\right)}. \tag{31}$$

One of the most important performance metrics that indicates how often wind turbines operate at their rated power across the year is the capacity factor (CF). It can be defined as the ratio of the actual energy produced by the wind turbine over a specific period to that produced should the turbine operate continuously at its rated power over the same period. For a specific site, CF can be approximated using the Weibull's distribution parameters, k and c, as follows [8]

$$CF = \frac{exp\left(-(\frac{v_{ci}}{c})^k\right) - exp\left(-(\frac{v_r}{c})^k\right)}{(\frac{v_r}{c})^k - (\frac{v_{ci}}{c})^k} - exp\left(-(\frac{v_{co}}{c})^k\right), \tag{32}$$

where the parameters v_{ci}, v_r, and v_{co} represent the wind turbine cut-in, rated, and cut-out velocities, respectively [8]. The wind turbine annual energy production (AEP) in kWh can be estimated using as follows:

$$AEP = 8760 \times CF \times P_r, \tag{33}$$

where P_r is the wind turbine rated power capacity in kW. In this study, the performance of eight different wind turbine models is assessed both technically and economically in the three investigated sites. Table 2 demonstrates the technical characteristics and the initial cost of the selected wind turbines. The economic feasibility of wind energy projects at a specific site depends largely on the energy conversion efficiency, capacity factor and initial costs of the selected wind turbines. The wind turbines listed in Table 2 offer a wide range in rated power capacity ranging from 600 - 2000 kW and initial cost that spans from 1000 to 4358 $/kW. Readers interested in further technical details of the selected wind turbine models (e.g., power curves, power generation technology, etc) can refer to [40], which is a website that offers a database of hundreds of wind turbine models from various manufacturers.

2.7. Economic performance

Similar to any electricity generating system, the economic viability of the wind energy turbines is dictated by minimizing the costs and maximizing the energy produced by the system. This can be readily evaluated by calculating the levelized cost of electricity (LCOE) in $/kWh which is the ratio of the total life cycle costs (TLCC) to the total life cycle energy production (TLCE)of the wind turbine [2],

$$LCOE = \frac{TLCC}{TLCE}. \tag{34}$$

Wind turbine total life cycle costs discounted to its present value using discounted cash flow method can be expressed as follows [2]:

$$TLCC = C_{inv} + \sum_{j=1}^{N} \frac{C_{O\&M}}{(1+D_r)^j} - \frac{B_{RV}}{(1+D_r)^N}, \tag{35}$$

where C_{inv} represents the project investment cost entailing the costs of the wind turbine hardware, mechanical and electrical installation costs. Whereas, N represents the useful lifespan of the wind turbines in years, selected in this study to be 25 years. Generally, the useful lifespan of wind turbines typically ranges from 20 to 25 years [41]. Nevertheless, with the recent advances in the wind turbine materials and performance monitoring and maintenance methods, wind turbines useful lifespan could be readily extended to 25 years and beyond [42]. Table 2 showcases the investment costs of the selected wind turbines in \$/kW. The parameter $C_{O\&M}$ represents the turbine fixed operation and maintenance costs. In this work, $C_{O\&M}$ is approximated to be 30% of the turbine investment cost [3]. The parameter B_{RV} models the residual value of the wind turbines, indicating the possible revenue obtained through selling wind turbine equipment and material after system decommissioning. The residual value is approximated as 10% of the wind turbine investment costs. The real discount rate, D_r, is estimated through correcting the nominal discount rate, D_o by the inflation rate, i, as follows [8]:

$$D_r = \frac{1 + D_o}{1 + i} - 1. \tag{36}$$

In this work, D_o and i are assumed to be 12% and 3%, respectively. The value of D_o is selected to approximately reflect the risk associated with such investments in Africa compared to their counterparts in North America and Europe, as outlined in [43]. The total life cycle energy produced by wind turbines discounted to its present value can be calculated as [10],

$$TLCE = \sum_{j=1}^{n} \frac{AEP}{(1 + D_r)^j}(1 - d_g)^j, \tag{37}$$

where d_g represents the wind turbine energy production degradation rate, which is assumed to be 1% on an annual basis. The system present value of benefits (PVB) which represents the total life cycle revenues collected through selling the produced electricity discounted to the present time is found as [8]

$$PVB = \sum_{j=1}^{n} \frac{E_p \times AEP}{(1 + D_r)^j}(1 - d_g)^j, \tag{38}$$

where E_p represents the price of electricity unit in \$/kWh paid by the customers. The profitability of the wind turbine can be assessed by determining the return on investment (ROI), which is calculated as [2]

$$ROI = \frac{NPV - C_{inv}}{C_{inv}} \times 100, \tag{39}$$

where NPV is the net present value of the project and it is evaluated by

$$NPV = TLCC - PVB. \tag{40}$$

Another economic metric used in evaluating the bankability of wind energy projects is the payback time (PB), which is the minimum time over which the wind energy project investment is recovered can be estimated by the following equation:

$$PB = -\frac{\log\left(1 - \frac{D_r C_{inv}}{B_A - C_{O\&M}}\right)}{\log\left(1 + D_r\right)}, \tag{41}$$

where B_A represents the yearly benefits derived from the sales of wind turbine-generated electricity. This can be computed as $B_A = E_p \times AEP$.

3. Results and discussion

3.1. Wind resource statistical analysis

3.1.1. Hourly, daily and monthly wind speeds

The wind resource which comprises wind speed and direction is assessed statistically in Aburin, Daarbuduq, and Xumba Weyne at various operating hub heights. The assessment includes analyzing wind speed variations on hourly, daily, monthly, and seasonally time frames. Additionally, annual and seasonal diurnal variations of wind speed are examined. As discussed in Section 2, the wind resource is a function of the site ambient temperature, air density, and the nature of surrounding landscape. As depicted in Fig. 3, the shear coefficient α varies across the year in all sites with minimum values observed during the dry hot months of the summer (June to August). Aburin experiences higher shear coefficient values which is due to the higher air density as a result of lower average ambient temperatures as shown in Fig. 3 (a). As depicted in Fig. 3 (c), the maximum monthly averaged shear coefficient in Aburin is found to be 0.31 in April, while the lowest is 0.24 in July. As for Daarbuduq and Xumba Weyne, the lowest monthly averaged shear coefficients occur in July and hey are found to be 0.23 and 0.21, respectively. The maximum monthly averaged shear coefficients are recorded in November as 0.32 and 0.31 for Daarbuduq and Xumba Weyne, respectively. It is evident that the summer months often witness the lowest average monthly shear coefficients. This could be attributed to the large variations in the diurnal surface temperatures. These variations result in large upward flow of air mass, leading to a less turbulent air and therefore lower values of shear coefficient.

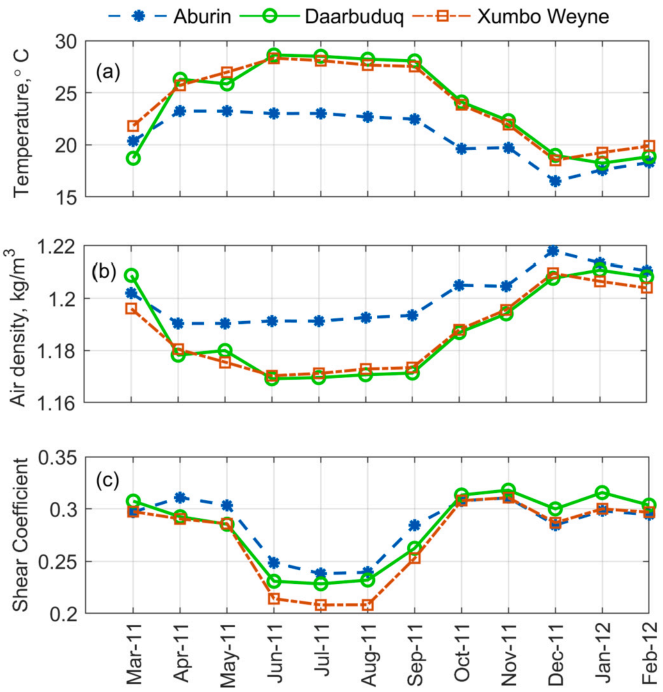

Fig. 3. Monthly variations in (a) ambient temperature (b) air density (c) shear coefficient for Aburin, Daarbuduq, and Xumba Weyne.

As shown in Fig. 4, the annual average wind speed in Aburin is 4.4 m/s, 4.9 m/s and 5.5 m/s for turbine hub height of 30 m, 50 m, and 80 m, respectively. That is approximately 20% increase in the annual mean wind speed between 30 m and 80 m hub heights. On an average daily basis, maximum estimated wind speed at 30 m hub height is 8.9 m/s with daily variance of 1.76 $(m/s)^2$. Whereas, on hourly time frame, the maximum estimated wind speed at the same hub height is 10.9 m/s with variance of 4.5 $(m/s)^2$. At 80 m hub height, the site experiences higher maximum hourly wind speeds of 12.9 m/s with higher variance of 6.3 $(m/s)^2$ as shown in Fig. 4 (c). As for Daarbuduq, a noticeable increase in the wind resource is observed compared to that of Aburin as shown in Fig. 5. The annual average wind speed in Daarbuduq is 4.5 m/s, 5.2 m/s and 5.8 m/s for turbine hub height of 30 m, 50 m, and 80 m, respectively. At a hub height of 80 m, the estimated maximum daily wind speed is 12.1 m/s with variance of 3.6 $(m/s)^2$. Whereas on hourly time frame, the site registers maximum wind speed of 14.7 m/s with hourly variance of 8.9 $(m/s)^2$. Significant increase in wind speed resource magnitude and variance is observed in Xumba Weyne as shown in Fig. 6. The annual average wind speed in Xumba Weyne is 5.1 m/s, 5.8 m/s and 6.2 m/s for turbine hub height of 30 m, 50 m, and 80 m, respectively. As demonstrated in Fig. 6 (c), the maximum average daily wind speed at hub height of 80 m is 14.2 m/s with corresponding variance of 6.2 $(m/s)^2$. High hourly wind variance of 12.4 $(m/s)^2$ is recorded in Xumba Weyne, which is approximately 28% more than that observed in Daarbuduq.

As for the wind direction, mainly two directions are prevalent in all the investigated sites, namely north east (NE) and south west (SW) as depicted in Fig. 7. The north easterly wind regime is generally less energetic compared to the south westerly wind regime across all three sites. Despite the fact that SW blowing winds are more energetic, the NE winds can not be overlooked. Careful evaluation needs to be conducted to design the wind turbine alignment and wind farm layout. This could entail using sophisticated yaw control system which would increase the capital cost of the system.

As shown in Fig. 8, the highest wind speeds in Aburin occur in the dry summer months, namely June, July, and August, in which July registered the peak monthly averaged wind speed of 7.8 m/s, 7.0 m/s, and 6.3 m/s for hub heights of 80 m, 50 m, and 30 m, respectively. The site experiences the lowest wind resource in the autumn months of October and November. Whereas, moderate wind speeds are prevalent across the rest of the months. As shown in Fig. 8, similar pattern is observed in both Daarbuduq and Xumba Weyne with noticeably higher wind speeds that reach up to 8.6 m/s and 10.3 m, respectively, at hub height of 80 m in July.

3.1.2. Diurnal wind speeds

The diurnal wind speed variation across the year and seasons is assessed. Fig. 9 demonstrates how the diurnal average wind speed varies across the year in the three sites under study. The highest wind speeds in Aburin occur between 9:00 to 11:00 AM, with slight drop in speed observed in the afternoon hours. Whereas, low speed winds blow during the night and early morning hours as depicted in Fig. 9 (a). Almost a similar pattern is observed in both Daarbuduq and Xumba Weyne, however the difference between the diurnal cycle peak and trough seem to be smaller, indicating a more uniform wind speeds in these two sites compared to that of Aburin as shown in Fig. 9 (b,c).

The annual diurnal patterns of wind speed shown in Fig. 9 indicate consistent wind speeds from 10:00 to 18:00, which partially coincides with the peak demand hours which typically occur between 16:00 to 20:00 for residential loads. The wind energy produc-

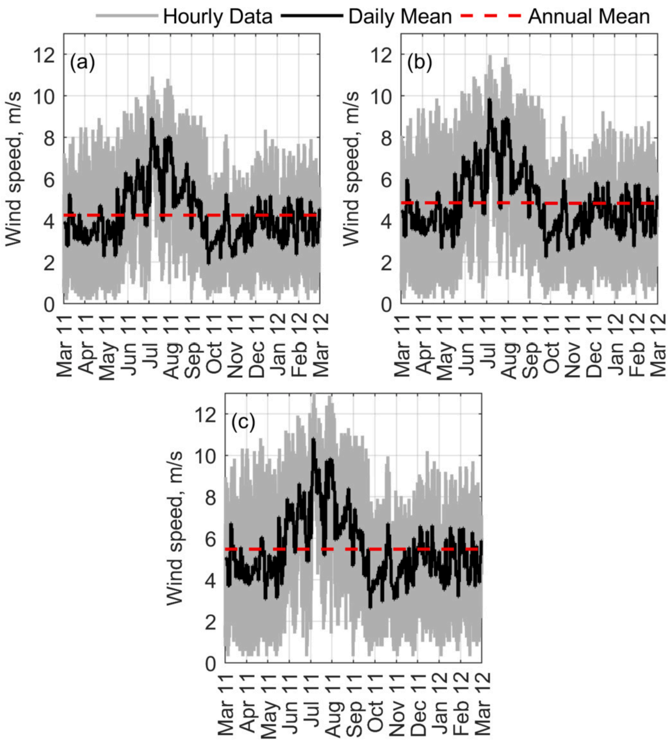

Fig. 4. Hourly, daily mean and annual mean of wind speed in m/s for Aburin at hub heights (a) 30 m (b) 50 m (c) 80 m.

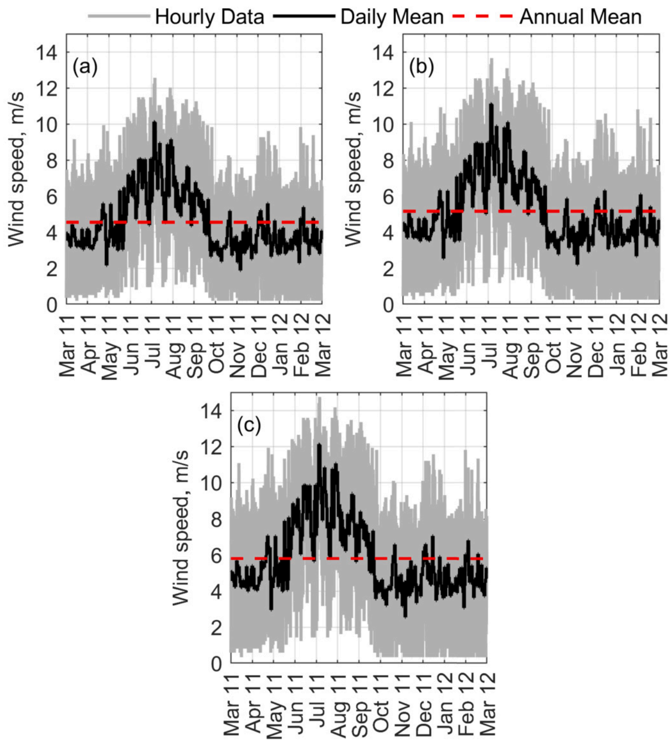

Fig. 5. Hourly, daily mean and annual mean of wind speed in m/s for Daarbuduq at hub heights (a) 30 m (b) 50 m (c) 80 m.

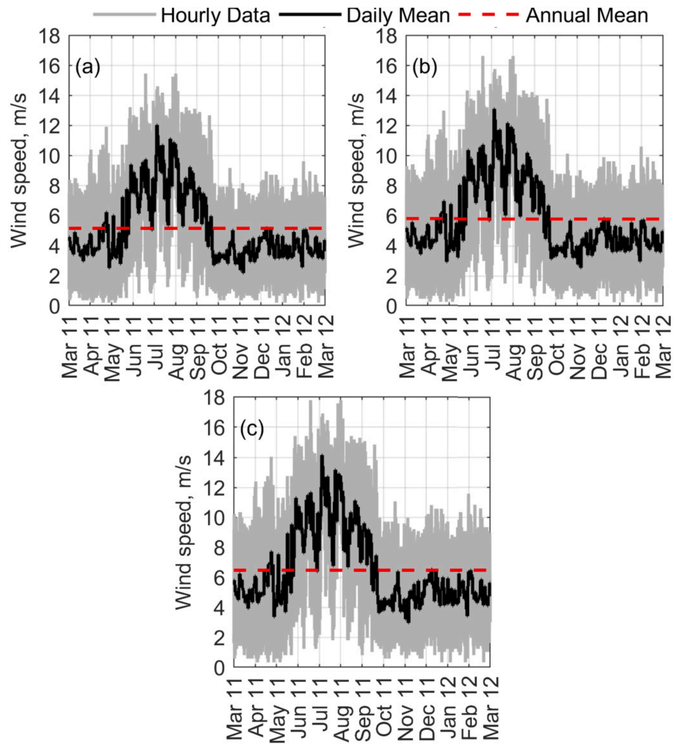

Fig. 6. Hourly, daily mean and annual mean of wind speed in m/s for Xumba Weyne at hub heights (a) 30 m (b) 50 m (c) 80 m.

Table 3
Weibull parameters for Aburin, Daarbuduq, and Xumba Weyne using four estimation methods at 10 m hub height.

Site	Estimation Method	k	c (m/s)	v_m (m/s)
Aburin		1.9514	3.6359	3.2245
Daarbuduq	EM	1.7613	3.9399	3.5083
Xumba Weyne		1.6100	4.4527	3.9899
Aburin		1.9021	3.2181	3.2181
Daarbuduq	MLE	1.6782	3.9122	3.4944
Xumba Weyne		1.5723	4.4454	3.9923
Aburin		1.8428	3.3505	3.0116
Daarbuduq	GM	1.5826	3.5706	3.2046
Xumba Weyne		1.6887	4.2728	3.8141
Aburin		1.9925	3.6375	3.2245
Daarbuduq	EPF	1.7979	3.9442	3.5083
Xumba Weyne		1.6343	4.4584	3.9899

tion curve can be shifted to better align with the daily peak demand by deploying storage systems such as battery energy storage systems (BESS). This is particularly necessary in the summer as the wind energy supply peaks around 10:00 in the morning and drops noticeably afterwards.

The seasonal diurnal cycles of the three sites at different operating hub heights are shown in Figs. 10-12. Peak diurnal wind speeds are observed during morning hours, typically between 9:00 to 11:00 AM, in both spring and summer seasons. The diurnal peak shifts to afternoon hours, between 2:00 to 6:00 PM, as the seasons transition to autumn and winter. In addition, the spring season features a more uniform diurnal cycle in the all the investigated sites compared to the other seasons. Autumn and winter seasons exhibit the highest variation between the peak and trough of the wind speed diurnal cycle. Furthermore, the summer months display steady wind speeds from early morning hours through midday.

3.2. Estimation of Weibull's parameters

The Weibull distribution function is fitted into the measured wind speed data by estimating the shape and scale parameters. As described in Section 2, four different parameter estimation techniques are deployed. Table 3 displays the estimated Weibull

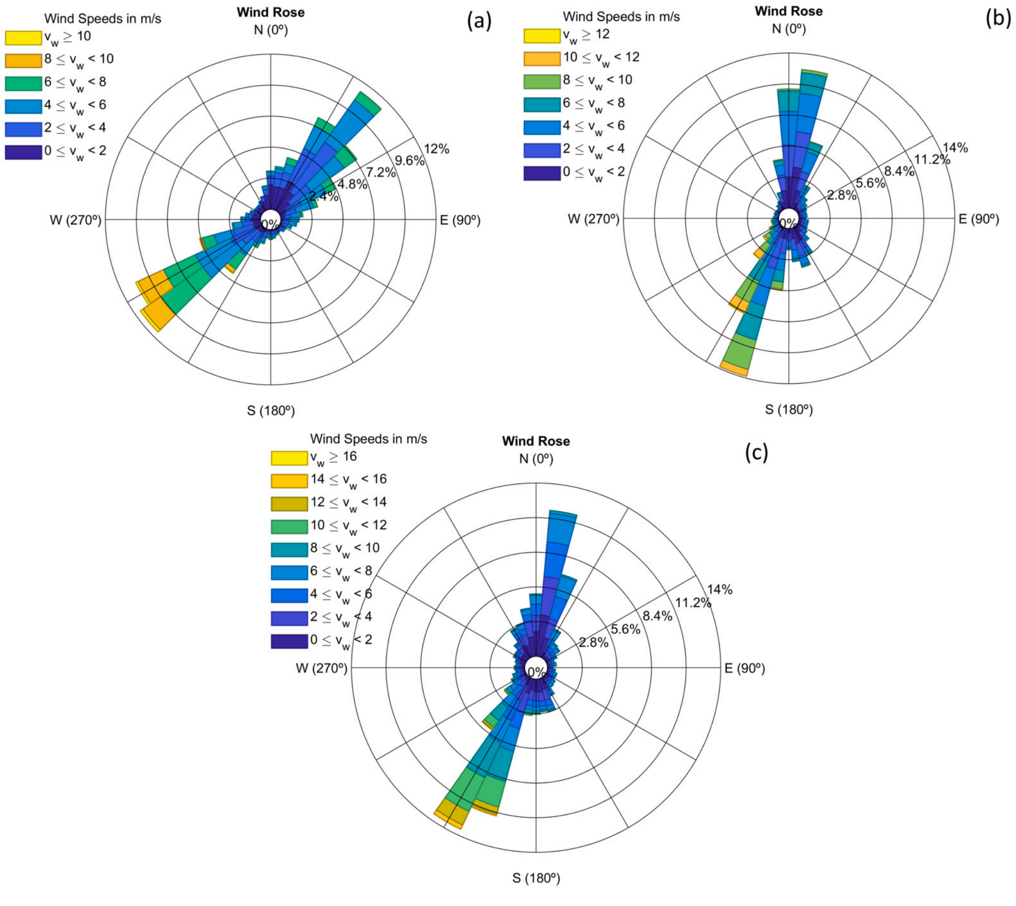

Fig. 7. Wind rose diagrams at hub height of 50 m (a) Aburin (b) Daarbuduq (c) Xumba Weyne.

Table 4
Statistical indicator for the goodness of fit in the three investigated sites for all four Weibull estimation methods at 10 m hub height.

Site	Estimation Method	RMSE	MAPE	RRMSE	MBE	R^2
Aburin	EM	0.0300	0.3621	2.3048	0.0003	0.8427
	MLE	0.0293	0.4074	2.2637	0.0004	0.8504
	GM	0.0359	0.3304	2.6935	0.0002	0.7753
	EPF	0.0309	0.3272	2.3581	0.0002	0.8332
Daarbuduq	EM	0.0239	0.4084	1.9723	0.0005	0.8520
	MLE	0.0224	0.4752	1.8674	0.0008	0.8700
	GM	0.0287	0.4378	2.3243	0.0006	0.7861
	EPF	0.0249	0.3806	2.0422	0.0004	0.8395
Xumba Weyne	EM	0.0295	0.5013	2.6545	0.0003	0.7702
	MLE	0.0286	0.5551	2.5832	0.0004	0.7846
	GM	0.0325	0.3831	2.8259	0.0001	0.7215
	EPF	0.0302	0.4723	2.7056	0.0003	0.7597

parameters using various estimation methods at typical anemometer measurement height (i.e., 10 m) in the three investigated sites. The goodness of fit for the four estimation methods are assessed in Table 4. It is clear that maximum likelihood estimation (MLE) method proved to produce the best fits with minimum RMSE values of 0.0293, 0.0224, and 0.0286 for Aburin, Daarbuduq, and Xumba Weyne, respectively. The MLE method also resulted in consistently high scores for the coefficient of determination R^2, that is 0.850, 0.870, and 0.7846 for Aburin, Daarbuduq, and Xumba Weyne, respectively. The poorest fit occurred in Xumba Weyne where the measured wind speed data feature bimodal distribution due to the variation in dominant wind speeds between the spring and summer seasons and autumn and winter seasons. Figs. 13-15 showcase the Weibull distribution functions estimated by various parameter estimation methods and at different hub heights for Aburin, Daarbuduq, and Xumba Weyne, respectively. Clearly Xumba

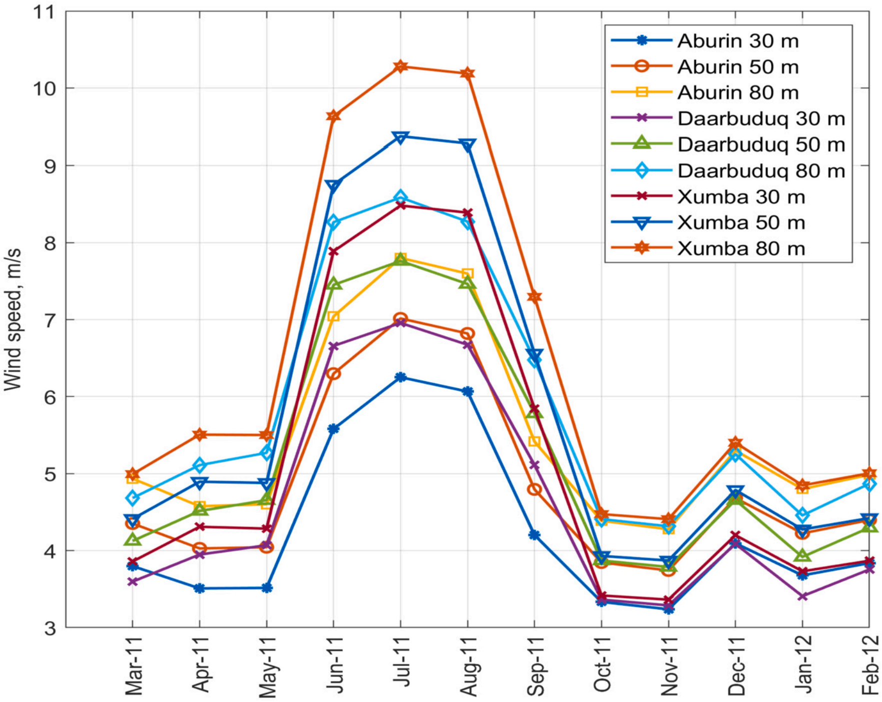

Fig. 8. Monthly averaged wind speed at 30 m, 50 m and 80 m hub heights in Aburin, Daarbuduq, and Xumba Weyne.

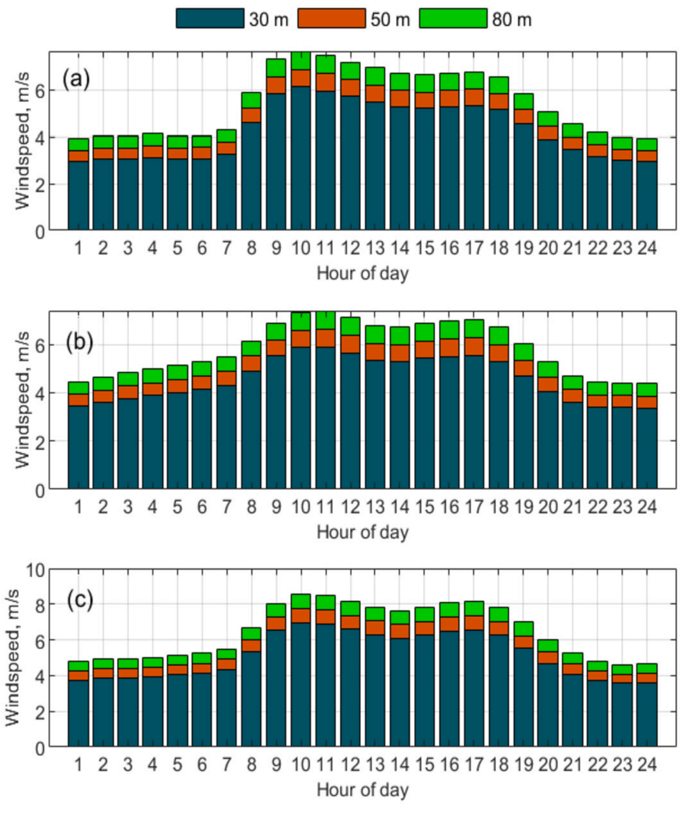

Fig. 9. Diurnal variation of wind speed across the year at different hub heights for (a) Aburin (b) Daarbuduq (c) Xumba Weyne.

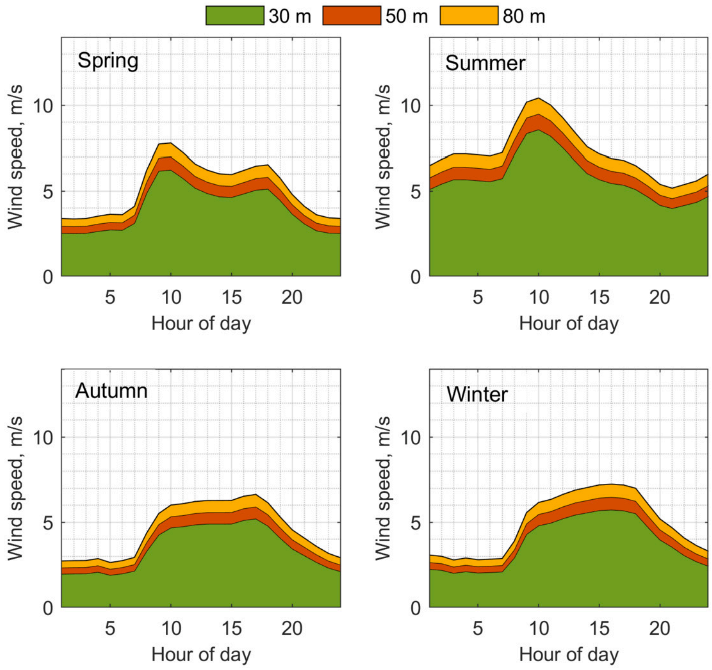

Fig. 10. Seasonal diurnal wind speed variation in Aburin.

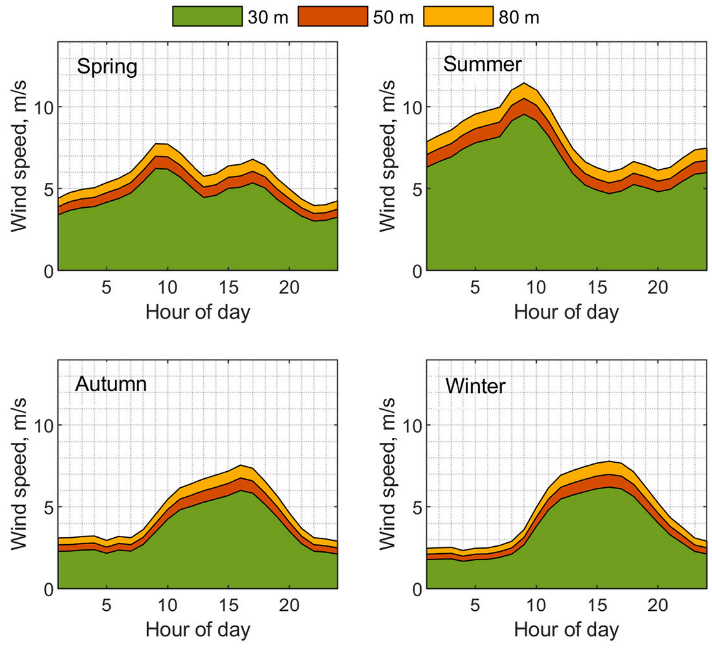

Fig. 11. Seasonal diurnal wind speed variation in Daarbuduq.

Weyne Weibull PDF exhibits higher likelihood for the occurrence of wind speeds greater than 6 m/s compared to Aburin and Daarbuduq.

3.3. Estimation of power and energy densities

One of the most crucial steps in assessing the potential of wind energy resource at a specific site is to estimate the power and energy densities. This helps not only for quantifying the available resource but also in the selection and sizing of wind turbines, wind farm layout, and ultimately the wind energy project economics. Tables 5 - 7 compare between the seasonal and annual power and

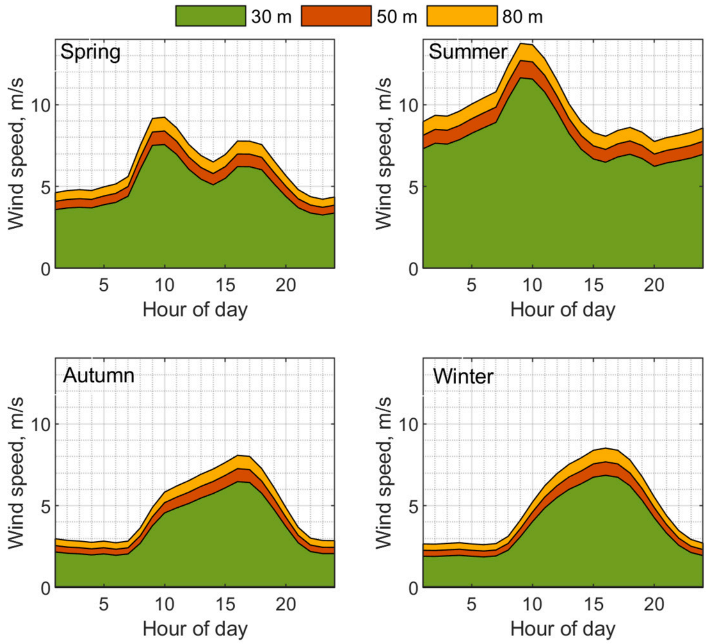

Fig. 12. Seasonal diurnal wind speed variation in Xumba Weyne.

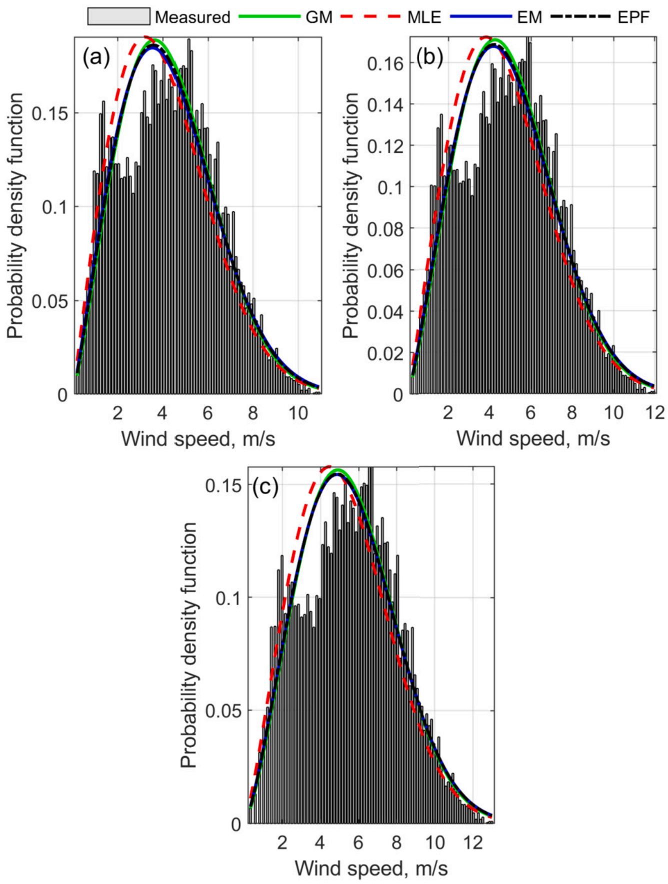

Fig. 13. Estimated wind speed Weibull PDF for Aburin at hub height (a) 30 m (b) 50 m (c) 80 m.

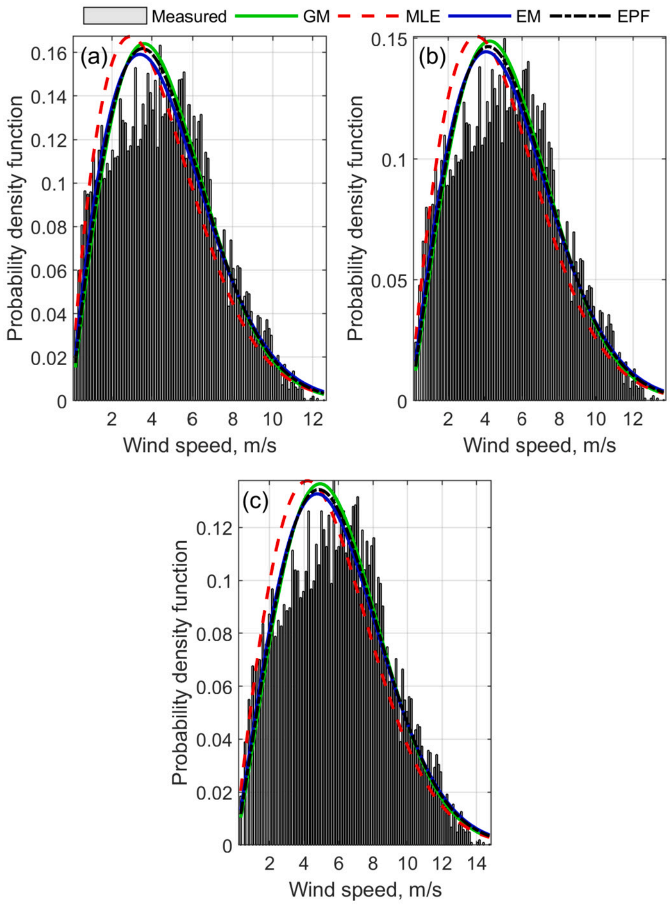

Fig. 14. Estimated wind speed Weibull PDF for Daarbuduq at hub height (a) 30 m (b) 50 m (c) 80 m.

energy densities for the three sites at different operating turbine hub heights. It also includes the MLE estimated Weibull function parameters, the mean wind speed, most frequent wind speed, and most energetic wind speed. In agreement with the aforementioned discussions, Xumba Weyne appear to have the highest annual power densities, that are, 179.30 kW/m^2, 241 kW/m^2, and 317 kW/m^2 for hub heights of 30 m, 50 m and 80 m, respectively. This corresponds to annual energy densities of 1573 kWh/m^2, 2115 kWh/m^2, 2782 kWh/m^2, respectively. It is also worth mentioning that more than 56% of the accessible wind energy is present during the summer in Xumba Weyne for the three investigated operating hub heights. In addition, autumn and winter seasons contain the least energy. Despite being approximately 50% lower in the annual energy density across all hub heights, Aburin is still enjoying moderate wind energy densities, that are 727 kWh/m^2, 1027 kWh/m^2, 1412 kWh/m^2, for the three considered hub heights, respectively.

As illustrated in Tables 5 - 7, more than 50% of the annual wind energy occurs exclusively in the summer season in all the three sites. This irregularity in the produced energy may pose challenges in matching the supply and demand at any given time across the year. This might signify the need to supplement wind power with other consistent energy sources such as solar PV arrays and diesel generators.

Tables 8-10 illustrate the wind power and energy densities for the three sites on monthly basis for hub heights of 50 m and 80 m. For hub height of 80 m, all three sites agree to have the highest energy and power densities in July, that are 259 kWh/m^2 (349 kW/m^2), 357 kWh/m^2 (480 kW/m^2), and 591 kWh/m^2 (794 kW/m^2), for Aburin, Daarbuduq, and Xumba Weyne, respectively. The months with the lowest energy and power densities are November for both Aburin and Daarbuduq, and January for Xumba Weyne as depicted in Tables 8-10.

3.4. Wind turbine performance

In this section, the techno-economic performances of eight different wind turbines described in Table 2 are examined for the three investigated sites. As shown in Table 11, the annual energy production (AEP) ranges from 0.35 GWh in Aburin using S47-660 turbine to 6.04 GWh in Xumbo Weyne using Enercon E66/1500 turbine. Consistent with earlier observations, all wind turbines show superior performance in Xumbo Weyne, followed with Daarbuduq, and subsequently Aburin. While not being the biggest turbine in nameplate power capacity, the Enercon E66/1500 turbine produced the highest annual energy in all the three locations with relatively high capacity factors. This is mainly due to the turbine high hub height (i.e., 86 m) and relatively wide turbine power curve, indicating

Table 5
Seasonal and annual wind power density (in W/m^2) and energy density (in kWh/m^2) along with the site characteristic wind speeds at a hub height of 30 m.

	Site	k	c (m/s)	v_m, v_f, v_e (m/s)	P_D (kW/m^2)	E_D (kWh/m^2)
Spring	Aburin	1.99	4.47	3.96, 3.14, 6.33	70.24	156.77
	Daarbuduq	2.07	5.04	4.47, 3.66 , 6.99	97.11	216.74
	Xumbo Weyne	1.79	5.57	4.95, 3.53 , 8.45	153.68	342.39
Summer	Aburin	3.19	6.48	5.80, 5.76, 7.55	156.74	349.69
	Daarbuduq	3.09	7.37	6.59, 6.49 , 8.66	233.18	520.45
	Xumbo Weyne	3.21	8.94	8.01, 7.96, 10.40	411.13	917.65
Autumn	Aburin	2.14	3.92	3.47, 2.92, 5.34	44.26	97.65
	Daarbuduq	1.77	4.07	3.62, 2.55, 6.23	60.97	132.37
	Xumbo Weyne	1.84	4.20	3.73, 2.74, 6.27	64.03	141.19
Winter	Aburin	2.20	4.29	3.80, 3.26, 5.75	56.52	105.76
	Daarbuduq	1.70	4.03	3.59, 2.37, 6.37	62.80	114.73
	Xumbo Weyne	1.84	4.32	3.84, 2.82, 6.44	69.53	130.16
Annual	Aburin	2.11	4.81	4.26, 3.54, 6.60	82.84	727.24
	Daarbuduq	1.90	5.20	4.60, 3.40, 7.60	116.50	1013.60
	Xumbo Weyne	1.70	5.80	5.10, 3.50, 9.00	179.30	1573.40

Table 6
Seasonal and annual wind power density (in W/m^2) and energy density (in kWh/m^2) along with the site characteristic wind speeds at a hub height of 50 m.

	Site	k	c (m/s)	v_m, v_f, v_e (m/s)	P_D (kW/m^2)	E_D (kWh/m^2)
Spring	Aburin	2.09	5.11	4.53, 3.75, 7.04	99.71	222.54
	Daarbuduq	2.18	5.73	5.08, 4.32, 7.73	135.92	303.37
	Xumbo Weyne	1.89	6.30	5.59, 4.23, 9.23	208.58	464.71
Summer	Aburin	3.36	7.28	6.53, 6.55, 8.37	217.85	486.01
	Daarbuduq	3.25	8.22	7.37, 7.34, 9.53	317.43	708.51
	Xumbo Weyne	3.40	9.90	8.90, 8.90, 11.30	544.70	1215.90
Autumn	Aburin	2.25	4.52	4.00, 3.48, 5.99	64.53	142.36
	Daarbuduq	1.87	4.68	4.15, 3.10, 6.91	86.59	187.98
	Xumbo Weyne	1.93	4.82	4.27, 3.30, 6.96	90.90	200.44
Winter	Aburin	2.32	4.92	4.36, 3.85, 6.43	81.52	152.53
	Daarbuduq	1.79	4.63	4.12, 2.93, 7.05	88.80	162.25
	Xumbo Weyne	1.94	4.95	4.39, 3.40, 7.14	98.32	184.05
Annual	Aburin	2.20	5.50	4.90, 4.20, 7.30	117.00	1026.90
	Daarbuduq	2.00	5.90	5.20, 4.10, 8.40	160.60	1397.80
	Xumbo Weyne	1.80	6.50	5.80, 4.20, 9.80	241.00	2115.20

Table 7
Seasonal and annual wind power density (in W/m^2) and energy density (in kWh/m^2) along with the site characteristic wind speeds at a hub height of 80 m.

	Site	k	c (m/s)	v_m, v_f, v_e (m/s)	P_D (kW/m^2)	E_D (kWh/m^2)
Spring	Aburin	2.20	5.78	5.12, 4.39, 7.76	137.79	307.54
	Daarbuduq	2.29	6.45	5.72, 5.02, 8.49	185.39	413.78
	Xumbo Weyne	1.98	7.06	6.26, 4.96, 10.03	276.69	616.46
Summer	Aburin	3.53	8.10	7.29, 7.37, 9.20	294.90	657.92
	Daarbuduq	3.41	9.10	8.17, 8.22, 10.41	421.62	941.07
	Xumbo Weyne	3.60	10.80	9.80, 9.90, 12.30	705.70	1575.10
Autumn	Aburin	2.37	5.14	4.56, 4.08, 6.66	91.38	201.58
	Daarbuduq	1.96	5.32	4.71, 3.69, 7.61	119.75	259.98
	Xumbo Weyne	2.03	5.47	4.85, 3.92, 7.67	125.67	277.09
Winter	Aburin	2.43	5.58	4.95, 4.49, 7.14	114.28	213.82
	Daarbuduq	1.88	5.27	4.68, 3.51, 7.75	122.36	223.56
	Xumbo Weyne	2.04	5.61	4.97, 4.03, 7.85	135.43	253.52
Annual	Aburin	2.30	6.20	5.50, 4.90, 8.10	160.80	1412.00
	Daarbuduq	2.10	6.60	5.80, 4.80, 9.20	216.20	1881.20
	Xumbo Weyne	1.90	7.30	6.50, 5.00, 10.60	317.00	2781.60

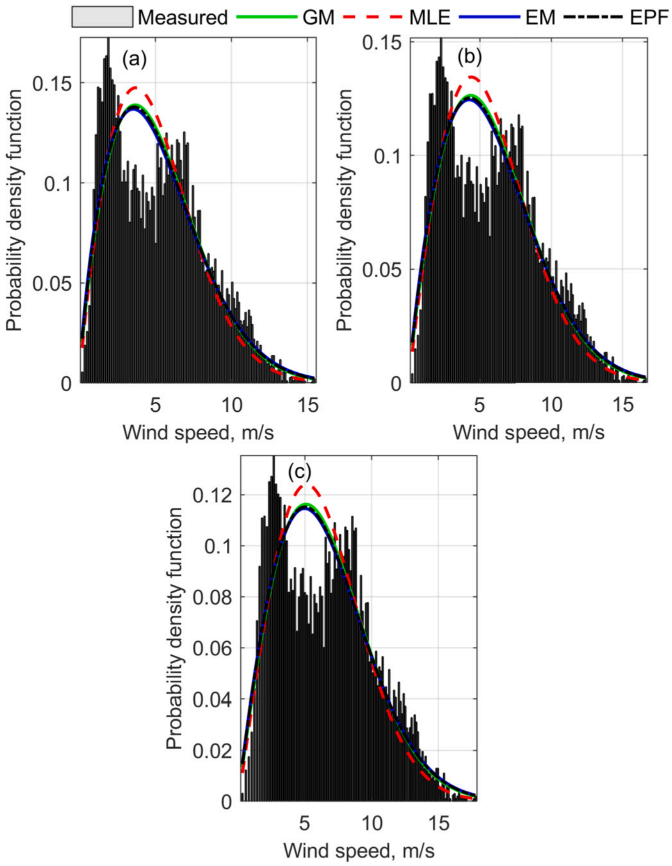

Fig. 15. Estimated wind speed Weibull PDF for Xumba Weyne at hub height (a) 30 m (b) 50 m (c) 80 m.

Table 8
Monthly wind power density (in W/m^2) and energy density (in kWh/m^2) in Aburin, along with the Weibull's estimated parameters at hub heights of 50 m and 80 m.

Month (Year)	Hub height = 50 m				Hub height = 80 m			
	k	c (m/s)	P_D (kW/m^2)	E_D (kWh/m^2)	k	c (m/s)	P_D (kW/m^2)	E_D (kWh/m^2)
March (2011)	2.17	4.91	85.52	51.31	2.28	5.57	119.26	71.56
April (2011)	1.82	4.52	80.75	58.14	1.91	5.15	111.90	80.57
May (2011)	2.14	4.57	69.84	51.96	2.25	5.20	98.28	73.12
June (2011)	3.67	6.98	187.03	134.66	3.86	7.78	255.61	184.04
July (2011)	3.68	7.78	259.05	192.74	3.87	8.63	348.54	259.31
August (2011)	3.82	7.55	234.62	174.55	4.02	8.38	317.44	236.17
September (2011)	2.31	5.41	108.94	78.32	2.42	6.11	150.56	108.25
October (2011)	2.18	4.35	59.40	44.14	2.29	4.97	84.33	62.66
November (2011)	2.33	4.22	51.18	36.80	2.45	4.82	73.39	52.77
December (2011)	2.58	5.28	93.78	69.77	2.71	5.97	131.14	97.57
January (2012)	2.30	4.77	74.67	55.48	2.42	5.42	105.09	78.09
February (2012)	2.27	4.97	85.35	59.40	2.38	5.63	119.27	83.01

greater power capturing capability. Furthermore, the Enercon E58/1000 turbine showcases the highest capacity factor (CF) values of 0.18, 0.24, and 0.31 at Aburin, Daarbuduq, and Xumbo Weyne, respectively. This underscores its efficiency in capturing a higher proportion of the available wind resources at all three locations. On the contrary, the S47-660 wind turbine records the least CF values of 0.06, 0.09, and 0.14 for the respective sites. Despite the fact that Enercon E53 wind turbine has greater hub height and more importantly higher rated power capacity (i.e., 60 m and 800 kW), Enercon E40 with 50 m hub height and 600 kW power rating managed to produce more annual energy yield in both Daarbuduq and Xumba Weyne. This seemingly counter-intuitive result can be attributed to the lower cut-in speed of Enercon E40 (i.e., 2.5 m/s) compared to Enercon E53 (i.e., 3 m). This advantage is lost in Aburin due to the lower wind speeds and the Enercon E53 higher power capacity might become more relevant.

Table 9
Monthly wind power density (in W/m^2) and energy density (in kWh/m^2) in Daarbuduq, along with the Weibull's estimated parameters at hub heights of 50 m and 80 m.

Month (Year)	Hub height = 50 m				Hub height = 80 m			
	k	c (m/s)	P_D (kW/m^2)	E_D (kWh/m^2)	k	c (m/s)	P_D (kW/m^2)	E_D (kWh/m^2)
March (2011)	1.86	4.65	85.77	51.46	1.95	5.29	118.65	71.19
April (2011)	2.14	5.10	96.90	69.77	2.25	5.77	134.25	96.66
May (2011)	2.51	5.24	93.45	69.52	2.63	5.93	130.55	97.13
June (2011)	3.82	8.25	306.33	220.56	4.01	9.12	409.17	294.60
July (2011)	3.40	8.65	363.63	270.54	3.58	9.54	480.42	357.43
August (2011)	3.42	8.32	323.24	240.49	3.60	9.20	429.55	319.59
September (2011)	2.49	6.52	180.84	130.21	2.61	7.30	244.67	176.16
October (2011)	1.88	4.35	69.09	51.13	1.97	4.96	96.63	71.51
November (2011)	1.81	4.24	66.69	47.21	1.91	4.84	93.24	66.02
December (2011)	1.78	5.20	126.38	90.36	1.87	5.89	171.18	122.39
January (2012)	1.80	4.37	74.40	54.39	1.89	4.99	103.42	75.60
February (2012)	1.84	4.81	95.58	64.81	1.94	5.46	131.48	89.14

Table 10
Monthly wind power density (in W/m^2) and energy density (in kWh/m^2) in Xumba Weyne, along with the Weibull's estimated parameters at hub heights of 50 m and 80 m.

Month (Year)	Hub height = 50 m				Hub height = 80 m			
	k	c (m/s)	P_D (kW/m^2)	E_D (kWh/m^2)	k	c (m/s)	P_D (kW/m^2)	E_D (kWh/m^2)
March (2011)	1.92	4.99	102.29	61.27	2.01	5.66	140.54	84.18
April (2011)	1.76	5.51	152.33	109.37	1.85	6.21	204.32	146.70
May (2011)	2.06	5.51	126.68	94.12	2.17	6.21	172.93	128.48
June (2011)	3.81	9.68	495.65	356.87	4.00	10.63	646.84	465.72
July (2011)	3.71	10.38	615.41	457.86	3.90	11.36	794.33	590.98
August (2011)	3.86	10.26	588.69	437.98	4.05	11.23	762.10	567.00
September (2011)	2.25	7.41	285.86	205.82	2.36	8.24	376.74	271.26
October (2011)	1.90	4.45	73.30	54.53	1.99	5.08	102.29	76.10
November (2011)	1.89	4.39	70.37	50.45	1.99	5.00	98.37	70.53
December (2011)	2.07	5.42	120.54	89.68	2.17	6.12	164.96	122.73
January (2012)	1.98	4.84	89.52	66.61	1.98	4.84	89.52	66.61
February (2012)	1.91	5.00	102.92	71.63	1.91	5.00	102.92	71.63

Economically, the Vestas V100 turbine offers the lowest LCOE, amounting to 0.080 $/kWh in Aburin, 0.059 $/kWh in Daarbuduq, and 0.044 $/kWh in Xumbo Weyne. In general, the S47-660 wind turbine exhibits the highest LCOE value in Aburin, standing at 0.166 $/kWh. Despite this, the cost remains notably lower than the existing local electricity generation costs within the country.

The economic analysis is extended by calculating the payback period for the chosen wind turbines across the three investigated locations. Fig. 16 (c) illustrates the payback time at a consistent nominal electricity selling price, E_p, of 0.15 $/kWh for all the selected wind turbines. According to Fig. 16 (c), wind turbines operating in Xumbo Weyne exhibit the shortest payback times, spanning less than 7.2 years. Conversely, wind turbines installed in Aburin have the lengthiest payback periods. Among the eight wind turbines that were selected, the Vestas V100 turbine stands out with the shortest payback times—4 years for Xumbo Weyne, 5.7 years for Daarbuduq, and 8.5 years for Aburin.

The profitability of the wind turbines is also assessed through examining the ROI% as shown in Fig. 16 (b). As expected, the turbines operating in Xumba Weyne yielded the highest ROI%, where Vestas V100 resulted in the highest ROI% among all analyzed wind turbines (i.e., 280%). Whereas, S47-660 deemed to be the least profitable with ROI% of 136%. All the examined wind turbines produced a positive ROI% except for S47-660 operating in Aburin, which resulted in a negative ROI%, indicating that the investment is incurring a loss rather than a profit.

3.5. Sensitivity analysis

A sensitivity analysis is conducted to explore how the economic viability of the selected wind turbines, as indicated by the project's key economic indicators, would be influenced by uncertainties in the prominent factors that impact wind turbine economics. Specifically, three variables, that are wind speed, discount rate, and the electricity selling price, are manipulated by ± 30% to generate a positive and negative effect on the LCOE, ROI% and PB of the Vestas V100 wind turbine, as illustrated in Fig. 17. The results presented in Fig. 17 (a) illustrates that in Xumbo Weyne, the LCOE exhibited a two-fold rise, approximately increasing from $0.04 to $0.08, as the wind speed profile at the site is reduced by 30% from its nominal values. Similarly, 30% decline in the wind resource in Aburin resulted in a substantial 177% increase in the LCOE for the selected wind turbine. In contrast, increasing the wind resource by 30% results in a relatively smaller change in the LCOE, that are 30% and 44% decrease in the LCOE for Xumba Weyne and Aburin, respectively as depicted in Fig. 17 (a). A more linear relationship is observed for the ROI% as the wind resource is varied as shown in Fig. 17 (b). The payback (PB) time varies non-linearly with variations in the wind resource as depicted in Fig. 17 (c).

Table 11
Annual energy production, capacity factor, and cost of energy using different wind turbines at Aburin, Daarbuduq, and Xumba Weyne.

Wind turbine	Hub height (m)	Site	k	c (m/s)	v_m (m/s)	AEP (GWh)	CF	LCOE ($/kWh)
WT1	80	Aburin	2.33	6.18	5.48	2.51	0.16	0.080
		Daarbuduq	2.05	6.58	5.84	3.41	0.22	0.059
		Xumbo Weyne	1.92	7.30	6.47	4.51	0.29	0.044
WT2	60	Aburin	2.26	5.74	5.09	1.42	0.13	0.133
		Daarbuduq	1.99	6.12	5.44	1.99	0.18	0.096
		Xumbo Weyne	1.87	6.82	6.05	2.70	0.25	0.070
WT3	60	Aburin	2.17	5.18	4.59	0.78	0.15	0.111
		Daarbuduq	1.91	5.53	4.92	1.08	0.21	0.082
		Xumbo Weyne	1.79	6.19	5.49	1.43	0.27	0.061
WT4	50	Aburin	2.22	5.48	4.86	0.60	0.15	0.114
		Daarbuduq	1.96	5.85	5.20	1.10	0.21	0.084
		Xumbo Weyne	1.83	6.53	5.79	1.45	0.28	0.063
WT5	70	Aburin	2.30	5.97	5.30	1.57	0.18	0.096
		Daarbuduq	2.02	6.36	5.65	2.11	0.24	0.073
		Xumbo Weyne	1.90	7.07	6.27	2.73	0.31	0.056
WT6	80	Aburin	2.33	6.18	5.48	2.66	0.15	0.114
		Daarbuduq	2.05	6.58	5.84	3.65	0.21	0.084
		Xumbo Weyne	1.92	7.30	6.47	4.83	0.28	0.063
WT7	86	Aburin	2.33	6.18	5.48	3.32	0.17	0.104
		Daarbuduq	2.05	6.58	5.84	4.56	0.23	0.078
		Xumbo Weyne	1.92	7.30	6.47	6.04	0.29	0.059
WT8	40	Aburin	2.17	5.18	4.59	0.35	0.06	0.166
		Daarbuduq	1.91	5.53	4.92	0.54	0.09	0.106
		Xumbo Weyne	1.79	6.19	5.50	0.82	0.14	0.070

Decreasing the wind speed by 30% in Xumba Weyne resulted in an increase in PB time from 4 years to 10 years. Even significant increase in PB time is noted in Aburin, that is from 8.5 years to 25 years (turbine life time).

Similarly, the nominal discount rate (D_o) is varied by ± 30% and the economic indicators are plotted for the three sites as shown in Fig. 17 (d-f). Decreasing D_o by 30% resulted in an almost linear drop in the LCOE of 25% for all the three sites. Slightly higher negative effect of 29% is observed when D_o is increased by 30% as illustrated in Fig. 17 (d). Decreasing D_o by 30% results in an increase in ROI% by 57% for Xumba Weyne and a slight drop in the PB time from 4 years to 3.7 years.

As shown in Fig. 17 (g), uncertainty in the electricity price (E_p) would not affect the LCOE since it does not factor in determining the TLCC and TLCE of the wind turbine. As for the ROI%, it is correlated linearly with the E_p as shown in Fig. 17 (h). Decreasing E_p has considerable effect on the PB time for less resourceful sites such as Aburin (73% increase) compared to more resourceful sites such as Daarbuduq and Xumba Weyne (55%) as demonstrated in Fig. 17 (i).

4. Conclusion

In this study, a thorough technical and economic assessment of wind energy potential in three selected sites in the western region of Somaliland is presented. The results obtained showcase that the wind energy potential in the three investigated sites are ranging from moderate to high potential. Xumba Weyne has the highest wind energy potential registering an annual average wind speed of 6.5 m/s and an annual most energetic wind speed of 10.6 m/s at an operating turbine hub height of 80 m. Following closely, Daarbuduq comes second with annual average wind speed of 5.8 m/s, and Aburin ranked third with an average wind speed of 5.5 m/s. The annual most frequent wind speeds are almost similar in the three investigated sites, however, substantial differences are observed in summer. The maximum likelihood estimation method proved to yield the lowest error between the measured and estimated wind speed data in all sites and for any time frame.

The results also underscore that deploying wind turbines with great hub heights and rotor swept areas is generally a safe choice, particularly for sites with moderate wind potential, such as Aburin. The S47-660 wind turbine resulted in the highest LCOE at 0.166 $/kWh in Aburin, yet it remains at 50% of the lowest electricity unit price in Somaliland (i.e., 0.3 $/kWh). Both Daarbuqud and Xumba Weyne are candidate potential sites for the development of wind energy farms that would serve the region of Maroodi Jeex, known to be the most densely populated region with the highest power demand. However, the absence of high voltage (HV) transmission lines and medium voltage (MV) distribution network presents technical and economic challenges that may impede the realization of such systems in Somaliland. More comprehensive studies need to be conducted in Somaliland to further characterize the wind energy resource in proximity to major demographic centers, optimize the design and layout of wind energy farms, accurately address system losses, and incorporate detailed economic analysis. Although limited historical wind speed data have been used in this study due to the significant scarcity of in-situ data, the results yielded valuable insights about the wind energy potential in the region

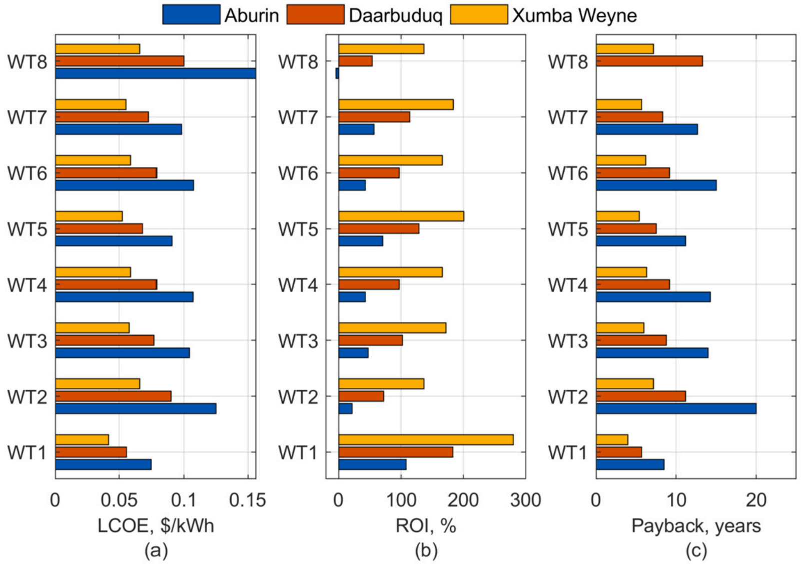

Fig. 16. The economic performance of the investigated commercial wind turbines at Aburin, Daarbuduq, and Xumba Weyne (a) LCOE (b) ROI% (c) Payback time.

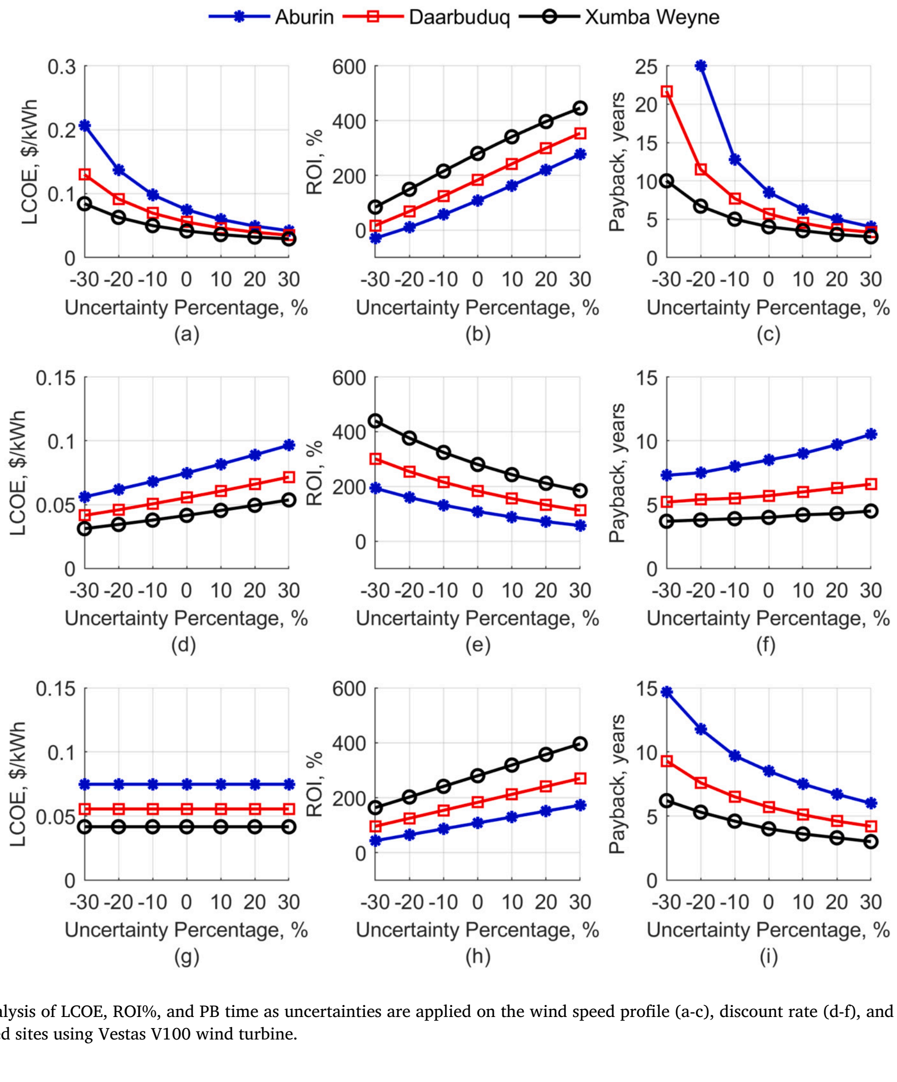

Fig. 17. Sensitivity analysis of LCOE, ROI%, and PB time as uncertainties are applied on the wind speed profile (a-c), discount rate (d-f), and electricity selling price (g-i) for the investigated sites using Vestas V100 wind turbine.

and established a solid benchmark for future comparative studies in this field. Such research endeavors would help in encouraging investors and assisting the government to make well-informed decisions.

Funding statement

This research did not receive any specific grant from any funding agency.

CRediT authorship contribution statement

Shaima Batran: Writing – original draft, Visualization, Investigation, Formal analysis, Data curation. **Mohamed Jama:** Writing – review & editing, Validation, Supervision, Resources, Project administration, Methodology, Investigation, Conceptualization. **Jawad Yousaf:** Writing – review & editing, Validation. **Taimur Hassan:** Validation, Formal analysis, Data curation. **Mohammed Ghazal:** Writing – review & editing, Validation. **Hazlie Bin Mokhlis:** Writing – review & editing, Validation.

Declaration of competing interest

The authors declare that they have no known competing financial interests or personal relationships that could have appeared to influence the work reported in this paper.

Data availability

Data will be made available on request.

Acknowledgement

The authors would like to thank Somalia Water and Land Information Management (SWALIM) | FAO Somalia for providing the ground station measurement data.

References

[1] IRENA, Renewable Capacity Statistics 2023, International Renewable Energy Agency, Abu Dhabi, 2023.
[2] J. Liu, S. Dongran, Q. Li, J. Yang, Y. Hu, F. Fang, Y. Joo, Life cycle cost modelling and economic analysis of wind power: a state of art review, Energy Convers. Manag. 277 (2023) 116628.
[3] IRENA, Renewable Power Generation Costs in 2022, International Renewable Energy Agency, Abu Dhabi, 2023.
[4] Kalam Azad, Mohammad Rasul, Pobitra Halder, J. Sutariya, Assessment of Wind Energy Prospect by Weibull Distribution for Prospective Wind Sites in Australia, 2019.
[5] Hossein Mohamadi, Alireza Saeedi, Zahra Firoozi, Saeid Sepasi Zangabadi, Shahla Veisi, Assessment of Wind Energy Potential and Economic Evaluation of Four Wind Turbine Models for the East of Iran, 2021.
[6] F. Fazelpour, E. Markarian, N. Soltani, Wind energy potential and economic assessment of four locations in Sistan and Balouchestan province in Iran, Renew. Energy 109 (2017) 646–667, https://doi.org/10.1016/j.renene.2017.03.072.
[7] M. Khaled, D. Bataineh, Assessment of wind energy potential for selected areas in Jordan, Renew. Energy 59 (2013) 75–81, https://doi.org/10.1016/j.renene.2013.03.034.
[8] M. Adnan, J. Ahmad, S. Ali, M. Imran, A techno-economic analysis for power generation through wind energy: a case study of Pakistan, Energy Rep. 7 (2021) 1424–1443.
[9] S. Ahmad, A. Al Rashid, S. Raza, A. Zaidi, S. Khan, M. Koç, Feasibility analysis of wind energy potential along the coastline of Pakistan, Ain Shams Eng. J. 13 (1) (2022) 101542, https://doi.org/10.1016/j.asej.2021.07.001.
[10] M. Gul, N. Tai, W. Huang, M.H. Nadeem, M. Yu, Assessment of wind power potential and economic analysis at Hyderabad in Pakistan: powering to local communities using wind power, Sustainability 11 (2019) 1391, https://doi.org/10.3390/su11051391.
[11] M. Sumair, T. Aized, S.A.R. Gardezi, S.U. Ur Rehman, S.M.S. Rehman, Wind potential estimation and proposed energy production in Southern Punjab using Weibull probability density function and surface measured data, Energy Explor. Exploit. 39 (6) (2021) 2150–2168, https://doi.org/10.1177/0144598720920748.
[12] Mukhtar M. Salah, Ahmed G. Abo-khalil, R.P. Praveen, Wind speed characteristics and energy potential for selected sites in Saudi Arabia, J. King Saud Univ., Eng. Sci. 33 (2) (2021) 119–128.
[13] Mohamad A. Alkhalidi, Shoug Kh. Al-Dabbous, S. Neelamani, Hassan A. Aldashti, Wind energy potential at coastal and offshore locations in the state of Kuwait, Renew. Energy 135 (2019) 529–539, https://doi.org/10.1016/j.renene.2018.12.039.
[14] Pham Quan, Thananchai Leephakpreeda, Assessment of wind energy potential for selecting wind turbines: an application to Thailand, Sustain. Energy Technol. Assess. 11 (2015) 17–26, https://doi.org/10.1016/j.seta.2015.05.002.
[15] Ali Wadi Al-Fatlawi, Maher A.R. Sadiq Al-Baghdadi, Hussain Togan, Goodarz Ahmadic, Saidur Rahman, Nasrudin Abd Rahim, Techno-Economic Analysis of Wind Turbines Powering Rural of Malaysia, 2022.
[16] Samuel Andres Gil Ruiz, Julio Eduardo Canon Barriga, J. Alejandro Martínez, Wind Power Assessment in the Caribbean Region of Colombia, Using Ten-Minute Wind Observations and ERA5 Data, 2021.
[17] Xinping Chen, Aoife Foley, Zenghai Zhang, Kaimin Wang, Kieran O'Driscoll, An Assessment of Wind Energy Potential in the Beibu Gulf Considering the Energy Demands of the Beibu Gulf Economic Rim, 2020.
[18] Pascalin Tiam Kapen, Marinette Jeutho Gouajio, David Yemele, Analysis and Efficient Comparison of Ten Numerical Methods in Estimating Weibull Parameters for Wind Energy Potential: Application to the City of Bafoussam, Cameroon, 2020, Reference 20.
[19] Kunal K. Dayal, John E. Cater, Michael J. Kingan, Gilles D. Bellon, Rajnish N. Sharma, Wind Resource Assessment and Energy Potential of Selected Locations in Fiji, 2021.
[20] Sneh Deep, Arnab Sarkar, Mayur Ghawat, Manoj Kumar Rajak, Estimation of the Wind Energy Potential for Coastal Locations in India Using the Weibull Model, 2021.

[21] Ivan Potic, Tatjana Joksimovic, Uros Milincic, Dusan Kicovic, Miroljub Milincic, Wind Energy Potential for the Electricity Production - Knjazevac Municipality Case Study (Serbia), 2021.
[22] Sangkyun Kang, Ali Khanjari, Sungho You, Jang-Ho Lee, Comparison of Different Statistical Methods Used to Estimate Weibull Parameters for Wind Speed Contribution in Nearby an Offshore Site, Republic of Korea, 2021.
[23] Younes El khchine, Mohammed Sriti, Performance Evaluation of Wind Turbines for Energy Production in Morocco's Coastal Regions, 2021.
[24] M. Hasan, P. Dey, S. Janefar, N. Salsabil, I. Khan, N. Chowdhury, A. Arefin, O. Farrok, A critical analysis of wind energy generation potential in different regions of Bangladesh, Energy Rep. 11 (2024) 2152–2173, https://doi.org/10.1016/j.egyr.2024.01.061.
[25] M. Elnaggar, H. El-Khozondar, M. Bashir, W. Salah, M. Al-Agha, M. Abudaqqa, A. El-mabhouh, Sustainable energy, economic, and environmental impacts of small-scale wind turbines: a comprehensive study, Int. J. Energy Res. 46 (8) (2022) 10808–10821, https://doi.org/10.1002/er.7881.
[26] H. Touria, C. Bouchra, Wind energy integration in Africa: development, impacts and barriers, Int. J. Electr. Comput. Eng. 12 (2022) 4614.
[27] Republic of Somaliland Ministry of Planning and National Development, National Development Plan III, Ministry of Planning and National Development, Hargeisa, Somaliland, 2023.
[28] Republic of Somaliland Ministry of Energy and Minerals, Environmental and Social Management Framework (ESMF) 2022, Ministry of Energy and Minerals, Hargeisa, Somaliland, 2022.
[29] M. Omer, Climate variability and livelihood in Somaliland: a review of the impacts, gaps, and ways forward, Cogent Soc. Sci. 10 (1) (2014) 2299108, https://doi.org/10.1080/23311886.2023.2299108.
[30] Republic of Somaliland Ministry of Environment and Rural Development, Strategic Plan (2017-2021), Ministry of Environment and Rural Development, Hargeisa, Somaliland, 2017.
[31] Paolo Billi (Ed.), Landscapes and Landforms of the Horn of Africa, Springer, 2022.
[32] S. Ullah, Territorial Diagnostic Report of the Land Resources of Somaliland, FAO-SWALIM, Nairobi, Kenya, 2016.
[33] R. Gore, B. Gawali, D. Pachpatte, Weather parameter analysis using interpolation methods, Artif. Intell. Appl. 1 (4) (2023) 260–272, https://doi.org/10.47852/bonviewAIA3202443.
[34] M. Lepot, J. Aubin, F. Clemens, Interpolation in time series: an introductive overview of existing methods, their performance criteria and uncertainty assessment, Water 9 (10) (2017) 796, https://doi.org/10.3390/w9100796.
[35] J.F. Manwell, J.G. McGowan, A.L. Rogers, Wind Energy Explained Theory, Design and Application, Wiley, 2009.
[36] Vladislovas Katinas, Mantas Marciukaitis, Giedrius Gecevicius, Antanas Markevicius, Statistical Analysis of Wind Characteristics Based on Weibull Methods for Estimation of Power Generation in Lithuania, 2017.
[37] Sunday Olayinka Oyedepo, Muyiwa S. Adaramola, Samuel S. Paul, Analysis of Wind Speed Data and Wind Energy Potential in Three Selected Locations in South-East Nigeria, 2012.
[38] Zahid Hussain Hulioa, Wei Jianga, S. Rehmanb, Techno - Economic Assessment of Wind Power Potential of Hawke's Bay Using Weibull Parameter: A Review, 2019.
[39] A. Shata, Investigation of wind characteristics and wind energy potential at Ras Ghareb, Egypt, Renew. Sustain. Energy Rev. 15 (6) (2011) 2750–2755, https://doi.org/10.1016/j.rser.2011.04.003.
[40] Wind Turbine Models, https://en.wind-turbine-models.com/turbines. (Accessed 2 January 2024).
[41] T. Adedipe, M. Shafiee, An economic assessment framework for decommissioning of offshore wind farms using a cost breakdown structure, Int. J. Life Cycle Assess. 26 (2021) 344–370.
[42] R. Wiser, M. Bolinger, Benchmarking Anticipated Wind Project Lifetimes: Results from a Survey of U.S. Wind Industry Professionals, Electricity Markets and Policy Group, Berkeley Lab., 2019.
[43] Grant Thornton LLP, Africa renewable energy discount rate survey – 2018, Grant Thornton, 2018.